

1 **Partitioning metabolism between growth and product synthesis for coordinated**
2 **production of wax esters in *Acinetobacter baylyi* ADP1**

3

4

5 **Suvi Santala^{1,2}, Ville Santala^{1,2}, Nian Liu¹, and Gregory Stephanopoulos^{1*}**

6

7 ¹Department of Chemical Engineering, Massachusetts Institute of Technology, Cambridge, MA 02139

8 ²Faculty of Engineering and Natural Sciences, Tampere University, Hervanta Campus, 33720 Tampere,

9 Finland

10 *Corresponding author gregstep@mit.edu

11

12

13

14 **Abstract**

15 Microbial storage compounds, such as wax esters (WE), are potential high-value lipids for the production
16 of specialty chemicals and medicines. Their synthesis, however, is strictly regulated and competes with
17 cell growth, which leads to trade-offs between biomass and product formation. Here, we use metabolic
18 engineering and synergistic substrate cofeeding to partition the metabolism of *Acinetobacter baylyi* ADP1
19 into two distinct modules, each dedicated to cell growth and WE biosynthesis, respectively. We first
20 blocked the glyoxylate shunt and upregulated the WE synthesis pathway to direct the acetate substrate
21 exclusively for WE synthesis, then we controlled the supply of gluconate so it could be used exclusively
22 for cell growth and maintenance. We show that the two modules are functionally independent from each
23 other, allowing efficient lipid accumulation while maintaining active cell growth. Our strategy resulted in
24 7.2- and 4.2-fold improvements in WE content and productivity, respectively, and the product titer was
25 enhanced by 8.3-fold over the wild type strain. Notably, during a 24-hour cultivation, a yield of 18% C-
26 WE/C-total-substrates was achieved, being the highest reported for WE biosynthesis. This work provides
27 a simple, yet powerful, means of controlling cellular operations and overcoming some of the fundamental
28 challenges in microbial storage lipid production.

29

30 Keywords: Microbial storage lipids, wax ester, substrate cofeeding, metabolic engineering

31 Introduction

32 Cells need carbon skeletons, energy, and reducing equivalents for their growth and product synthesis.
33 Despite being an oversimplification, this basic concept illustrates that the biological functions of cells
34 depend on these key components, which are all derived from available nutrients in the surrounding
35 environment. Cellular metabolism has evolved to optimally generate these components for growth, yet
36 this optimum is perturbed when cells are engineered to generate a product, especially when the
37 production pathway is overexpressed. Consequently, metabolic engineering, which targets the integrated
38 function of all pathways, aims to attain a new balance that best partitions the resources from carbon
39 sources between growth and product synthesis by rewiring pathway fluxes. However, commonly used
40 substrates such as glucose pose specific challenges as it can be consumed by a multitude of extraneous
41 pathways that may result in lower yields. Other industrially favored substrates, such as acetate which can
42 be readily produced from natural gas, anaerobic digestion, or CO₂ fixation, can create additional
43 complications due to potential imbalances in the supply and demand of carbon, energy, and cofactors.

44 The issues outlined above are exacerbated in the production of highly reduced compounds from
45 energetically inferior substrates, exemplified by the production of lipids from acetic acid. When acetate is
46 used as a sole carbon source, it is directed to the growth-related tricarboxylic acid (TCA) cycle and
47 glyoxylate shunt instead of production pathways to provide critical components for the cell. Redirecting
48 acetate to product synthesis introduces non-trivial perturbations in metabolism that may be resisted by
49 innate cellular regulatory mechanisms. Dynamic regulation of pathways can help address these issues by
50 autonomously controlling the flux distribution towards biomass and product (Kent & Dixon, 2020; Lalwani,
51 Zhao, & Avalos, 2018). For example, in order to enhance acetate to wax ester (WE) conversion, Santala et
52 al. previously described an autonomous circuit that dynamically regulated the expression of isocitrate
53 lyase encoded by *aceA* in the glyoxylate shunt (Santala, Efimova, & Santala, 2018), enabling the optimal

54 distribution of carbon between cell growth and WE synthesis in *Acinetobacter baylyi* ADP1. Bypassing
55 native regulations improved the WE yield from acetate by up to four-fold, and allowed the cells to
56 accumulate 19% of their cell dry weight (CDW) as WEs. However, the engineered cells exhibited reduced
57 growth and volumetric productivity compared to the wild type, potentially due to limited supply of energy
58 and reducing equivalents. Other strategies have involved growth coupling, decoupling, or reward-
59 punishment-based feedback circuits to boost metabolic activity, cell fitness, and bioprocess
60 competitiveness (Burg et al., 2016; Lo, Chng, Teo, Cho, & Chang, 2016; Lv et al., 2019; Mehrer et al., 2019;
61 von Kamp & Klamt, 2017). Despite these advances, simultaneously satisfying the biosynthetic
62 requirements of both cell growth and product formation still remains a major challenge.

63 One way to resolve the conflicts between growth and production is to separate the two processes
64 temporally, as demonstrated in the microbial synthesis of lipids which includes triacylglycerols (TAGs) and
65 WEs. These compounds are highly carbon and cofactor intensive, and they compete strongly with biomass
66 for cellular resources. Furthermore, lipid production is strictly regulated and requires nutrient limitations
67 that allow the carbon flux to be diverted towards lipids instead of biomass (Beopoulos et al., 2009; Fixter,
68 Nagi, McCormack, & Fewson, 1986), implying that production is maximized when growth rate is near zero
69 (Yan & Pfleger, 2020). These conditions are implemented in practice by providing excess glucose but
70 limited nitrogen (high C/N ratios), thereby limiting growth once nitrogen is depleted. As a result, growth
71 occurs first in this two-phase process and is then followed by subsequent lipid accumulation (Kurosawa,
72 Boccazzi, de Almeida, & Sinskey, 2010; Xu, Zhao, Du, & Liu, 2017). Nevertheless, such approaches limit the
73 flexibility needed for cell regeneration and results in lower overall yield and productivity.

74 To better fulfill the biosynthetic requirements of both growth and the production pathway, Park et al.
75 employed a dual-substrate co-feeding strategy. With acetate as the main carbon source they also
76 provided the cells with an additional carbon source, gluconate, that was fed to the reactor in a controlled
77 and optimized manner, circumventing catabolite repression (Park et al., 2019). Gluconate as the preferred

78 carbon source supplied reducing equivalents while acetate, the primary yet non-preferred carbon source,
79 supplied ATP and carbon skeletons. This synergistic substrate cofeeding facilitated the generation of ATP
80 and reducing equivalents more efficiently compared to the sole use of either single substrate. As a result,
81 the metabolic productivity achieved by the synergistic substrate cofeeding exceeded the sum of individual
82 substrate productivities (Park, et al., 2019).

83 Here, by employing both metabolic engineering and substrate cofeeding, we address the fundamental
84 issues of both unbalanced supply of biochemical resources and the trade-off between growth and
85 production in the context of microbial lipid synthesis. Combining the advantages of each approach, we
86 show that it is possible to grow biomass and simultaneously maximize the synthesis of a secondary
87 product, which is demonstrated by the superior WE formation in *A. baylyi* ADP1, a model host for studying
88 WE production in bacteria (Ishige, Tani, Sakai, & Kato, 2003; Luo, Efimova, Losoi, Santala, & Santala, 2020;
89 Santala, Efimova, Koskinen, Karp, & Santala, 2014; Stöveken, Kalscheuer, Malkus, Reichelt, & Steinbüchel,
90 2005). Metabolic engineering was used to force the primary carbon source, acetate, to the WE synthesis
91 pathway, while the cofeeding of gluconate as a secondary dopant substrate supported the synthesis of
92 cofactors and all other necessary cell components.

93 **Materials and Methods**

94 **Strains and media**

95 *Acinetobacter baylyi* ADP1 (DSM 24193, DSMZ, Germany) wild type and *A. baylyi* ADP1 Δ *acr1::Kan^r/tdk*
96 Δ *aceA::P_{T5}-acr1-spec^r* (Luo, et al., 2020) (ADP1m+) were used in the study. Cultivations for all experiments
97 were carried out using minimal salts medium (MSM) (Hartmans, Smits, van der Werf, Volkering, & de
98 Bont, 1989) supplemented with Na-gluconate and/or Na-acetate where appropriate. All pre-cultivations
99 were done in MSM supplemented with 0.1% casein amino acids, 50 mM Na-acetate, and 50 mM Na-

100 gluconate. Kanamycin ($30 \mu\text{g mL}^{-1}$) and streptomycin (or spectinomycin) ($50 \mu\text{g mL}^{-1}$) were added for
101 ADP1m+ in all cultivations.

102 **Flux balance analysis**

103 Flux balance analyses (FBA) were carried out with the COBRApy Python package (version 0.13.3) (Ebrahim,
104 Lerman, Palsson, & Hyduke, 2013). The FBA was used to calculate the theoretical yields of the conversion
105 of gluconate and acetate into WEs by ADP1. A previously described genome-wide *A. baylyi* metabolic
106 network (Durot et al., 2008) was used for its implementation with an added exchange reaction for WEs.
107 In order to predict the optimal consumption of gluconate and acetate in terms of biomass and WE
108 production, the growth reaction was first maximized per available substrates. Thereafter, the residual
109 acetate was calculated and the WE accumulation was maximized per available acetate. In all FBA analyses,
110 the model was given a total of $1 \text{ g gCDW}^{-1} \text{ h}^{-1}$ of carbon source mixtures at different ratios as inputs with
111 default minimal medium components and unlimited oxygen.

112 **Batch cultivations**

113 In all cultivations, initial OD_{600} was 0.1 – 0.3. The initial batch cultivations performed for analyzing the
114 tolerance and consumption of acetate were done as two parallel 5 ml cultivations at $30 \text{ }^\circ\text{C}$, 250 rpm for
115 48 h. The medium was supplemented with 50 mM Na-gluconate and Na-acetate (0, 10, 50, or 100 mM).
116 To test the ability of the engineered strain to consume acetate as the sole carbon source, similar growth
117 conditions were used, except without gluconate supplementation. Growth based on optical density
118 (absorbance at 600 nm) and consumption of substrates were determined after 24 and 48 hours. The initial
119 tests for investigating simultaneous consumption of gluconate and acetate were done as two parallel
120 cultivations in a 50 mL medium in 250 mL shake flasks at $30 \text{ }^\circ\text{C}$ and 250 rpm for 47 hours. MSM was
121 supplemented with 100 mM Na-gluconate and 100 mM Na-acetate.

122 **Bioreactor experiments**

123 Small volume (60 mL) fed-batch cultivations were carried out in 250 ml bioreactors (Applikon
124 Biotechnology, Netherlands) at 30°C, 350 rpm, and an airflow of 1 vvm. In all cultivations, an initial optical
125 density OD₆₀₀ of 0.1 – 0.3 was used. Acetate (70 - 100 mM) and gluconate (2 mM) were supplemented as
126 batch and additional gluconate was fed to the vessel at feed rates of 0.1 – 0.8 mM h⁻¹ using a constant
127 volumetric flow rate with varying gluconate concentrations. Acetate was not included in the control
128 cultivation. Dissolved oxygen and pH were on-line monitored during the cultivations. Samples for biomass
129 determination (optical density) and substrate consumption were taken manually. For the ¹³C isotopic
130 tracing experiments, [U-¹³C₂]acetate was used (99%; Cambridge Isotope Laboratories, USA).

131 Large volume (500 mL) fed-batch cultivations were carried out in 1 L bioreactors (Biostat B, Sartorius,
132 Germany) at 30°C and the airflow was set to 1 vvm. An initial optical density OD₆₀₀ of 0.3 was used. Acetate
133 (50-75 mM) and a small amount of gluconate (2 mM) was supplemented as batch and a feed solution
134 containing 25 mM gluconate and 25 mM acetate was fed to the vessel at rates of 1.15 mL h⁻¹ (T2) and 6.9
135 mL h⁻¹ (T3). The dissolved oxygen, pH, and optical density were on-line monitored during cultivation. The
136 partial oxygen pressure was adjusted to 20% by stirring cascade (100 – 350 rpm), and pH was adjusted to
137 7.5 by H₃PO₄ and NaOH. The samples for substrate consumption and WE analyses were taken manually.

138 **Lipid analyses**

139 Methods for lipid and metabolite analyses are described in Supporting Information.

140 **Results**

141 We partitioned cell metabolism into two distinct modules, one fueled by acetate and dedicated to WE
142 synthesis and another utilizing gluconate for the synthesis of cofactors and biomass precursors (Figure 1).
143 We aimed to achieve the growth-production scheme indicated in Figure 1B. To achieve this partition, we
144 employed a strain in which isocitrate lyase (*aceA*) is deleted. This deletion eliminates glyoxylate shunt,
145 which is essential for growth on acetate; the lack of glyoxylate shunt prevents the cells to bypass the two

146 decarboxylation steps of TCA cycle that yield CO₂, and therefore carbon from acetate cannot be rerouted
147 for the synthesis of cell components through gluconeogenesis and the pentose phosphate pathway (PPP)
148 (Barbe et al., 2004; Santala, et al., 2018). In addition, to enhance the flux of acetate towards WE synthesis,
149 the native fatty acyl-CoA reductase Acr1, which is a key enzyme for WE production (Lehtinen, Efimova,
150 Santala, & Santala, 2018; Reiser & Somerville, 1997), was replaced with a constitutively expressed Acr1
151 (Luo, et al., 2020). With these modifications, the engineered strain, designated as ADP1m+, was unable to
152 grow in minimal salts medium (MSM) using acetate as the sole carbon source. Furthermore, when cells
153 were first cultivated on gluconate and subsequently transferred to acetate medium, they were not able
154 to efficiently utilize acetate for continued WE synthesis, presumably due to limited cofactor availability
155 (Supplementary Figure S1).

156 Next, the ability of the strain to tolerate and consume acetate in the presence of glycolytic substrates was
157 investigated. Simultaneous consumption of gluconate and acetate was detected for both ADP1m+ and
158 ADP1 wild type (WT) in batch cultures (Figure 2A), indicating that the utilization of acetate by ADP1m+ is
159 not impaired in the presence of gluconate. In addition, ADP1m+ produced more WEs than ADP1 WT in
160 the studied conditions (Figure 2B). Notably, providing the cells with excessive amounts (100 mM) of
161 gluconate resulted in a yellow coloring of the supernatant, indicating that some of the carbon was directed
162 to the synthesis of extracellular substances, such as exopolysaccharides (EPS), which are typically
163 produced by *Acinetobacter* spp. when grown on excess of glycolytic substrates (Kannisto, Efimova, Karp,
164 & Santala, 2017; Kaplan & Rosenberg, 1982) (Supplementary Figure S2).

165 Although the engineered strain simultaneously consumed acetate and gluconate, it was not clear to what
166 extent the lipids were synthesized from acetate relative to gluconate. To elucidate the carbon partitioning,
167 ADP1m+ was cultivated in MSM with natural abundance gluconate and [U-¹³C₂]acetate (Figure 3), with
168 both substrates being available in excess at the time of sampling. Isotopic tracing for central carbon
169 metabolites as well as fatty acyl methyl esters (FAMES) derived from cellular lipids revealed that glycolytic

170 and PPP metabolites were completely unlabeled and, hence, were generated from gluconate, whereas
171 ~90% of lipids were labelled, indicating a dominant contribution to lipid synthesis from acetate.

172 The result above suggested that cell growth could be separated from WE production by adjusting the
173 availability of acetate and gluconate in the culture medium. To investigate this possibility, cultivations
174 with different gluconate feed rates (0.8; 0.4; 0.2; 0.1 mM h⁻¹) in MSM were carried out for the engineered
175 strain (Figure 4). In these experiments, the MSM contained 70–100 mM Na-acetate and 2 mM gluconate
176 initially. In addition, a cultivation without acetate (0.4 mM h⁻¹ gluconate feed only) was carried out as a
177 control.

178 At the 0.8 mM h⁻¹ feed rate, gluconate accumulated in the medium as it was supplied at a rate faster than
179 it was consumed by the cells. As ADP1m+ cannot assimilate acetate for growth, gluconate availability
180 controlled cell growth at feed rates 0.4, 0.2, and 0.1 mM h⁻¹; after the cultures reached a cell density
181 where gluconate was limiting (concentration in the culture remained at 0 mM), cell growth became
182 'carbon-limited' despite the presence of excess amounts of acetate in the culture. This carbon-limited
183 growth mode was also indicated by the observed linear growth and partial oxygen pressures
184 (Supplementary Figure S3). For comparison, cultivations with 0.8 mM h⁻¹ gluconate was also conducted
185 with ADP1 WT (Supplementary Figure S4). As expected, the wild type cells did not exhibit carbon-limited
186 growth, as the cells can fully utilize acetate when gluconate was scarce (Supplementary Figure S4).
187 Partitioned metabolism with acetate and gluconate substrates in ADP1m+ was retained in gluconate-
188 limiting conditions as confirmed by isotopic tracing using [U-¹³C₂]acetate (Supplementary Figure S5).

189 Higher gluconate availability resulted in better gluconate consumption, consistent with the increased cell
190 density at the end of the culture (Figure 4). By reducing the gluconate feed rate, the fraction of acetate
191 consumed among the total pool of substrates increased from 49% (w/w) at 0.8 mM h⁻¹ gluconate feed, to
192 74% at 0.1 mM h⁻¹ gluconate feed. Interestingly, no drastic changes were observed in the amount of

193 synthesized WEs under all these conditions despite the major reduction in gluconate availability (Figure
194 4), consistent with the hypothesis of segregated cellular operations for cell growth and WE production.
195 Hence it was concluded the amount of gluconate can be reduced without negatively affecting WE
196 production in ADP1m+. Furthermore, in the control cultivation without acetate, ADP1m+ did not produce
197 detectable amounts of WE, suggesting that gluconate at the applied feed rate (0.4 mMh^{-1}) was not
198 sufficient for WE synthesis. Taken together, these results indicated that in ADP1m+ acetate served as the
199 exclusive carbon source for WE synthesis, while gluconate was essential for cell growth and maintenance
200 (Figure 5).

201 There is clearly an optimum in the consumed acetate/gluconate ratio. Too little gluconate will not allow
202 sufficient growth and result in low volumetric WE accumulation. On the other hand, too much gluconate
203 will yield higher biomass but with lower WE content and carbon yield. To determine the optimal
204 acetate/gluconate ratio that maximizes total WE accumulation we carried out flux balance analysis (FBA)
205 for the *aceA* deficient *A. baylyi* ADP1 (Supplementary Figure S6). According to the model, biomass
206 production is not affected if acetate consumption accounts for less than 50% of the total substrate
207 consumption (set to a max of $1 \text{ gCDW}^{-1} \text{ h}^{-1}$). However, if acetate consumption is above 50% of the total
208 substrate uptake, the biomass production decreases linearly with increasing acetate; if all of the
209 consumed substrate is acetate, then no biomass production occurs. In contrast, accumulation of WEs
210 strongly increases along with increasing proportion of acetate in total substrate consumption. FBA results
211 suggested that a ratio of approximately 75% acetate and 25% gluconate taken up by the cells would be
212 optimal in terms of simultaneously maximizing both biomass and WE production per consumed carbon.
213 Correspondingly, the lowest gluconate feeding rate of 0.1 mM h^{-1} in previous experiments was selected
214 as it gave a consumption ratio that is closest to the calculated optimum (74% acetate and 26% gluconate).
215 To test the FBA prediction, we cultured the engineered strain in larger scale bioreactors (1 L in size with
216 500 ml working volume) with pH and pO_2 control. Batch media conditions similar to the previous

217 cultivations were employed, and runs with two different gluconate feeding rates, 0.6 mM h⁻¹ (T2) and 0.1
218 mM h⁻¹ (T3), were conducted (Figure 6). To ensure sufficient acetate supplementation throughout the
219 cultivation, acetic acid was added to the feed in the same concentration as gluconate. For comparison, a
220 cultivation of the WT strain under conditions similar to T3 was also carried out (Supplementary Figure S7).

221 In T2, ADP1m+ exhibited exponential growth until gluconate was no longer in excess, thus allowing higher
222 biomass accumulation in the beginning of the cultivation (Figure 6A). The cells shifted to linear growth
223 after ~10 h as the gluconate feed rate could no longer keep up with the total consumption rate. At the 9
224 h timepoint, a total of 13 mM acetate (including the fed acetic acid) and 6.8 mM gluconate were
225 consumed, and the WE content reached 13%, as determined by nuclear magnetic resonance spectroscopy
226 (NMR), demonstrating that lipid accumulation was efficient already in the early stages of the culture.

227 Cultivation was stopped at 22 h in order to avoid acetate limitation (~2 mM acetate remained). At the end
228 of cultivation, the total biomass in the system was 1.7 g L⁻¹ and the WE content had increased to 20%,
229 corresponding to a productivity of 15 mg WE L⁻¹ h⁻¹ (Figure 6C). The amount of substrate consumed was
230 12 mM for gluconate and 46 mM for acetate (including both initial and fed acetic acid), resulting in acetate
231 accounting for 54 % (w/w) of total substrate use. The C/C yield for WEs was 14%, which was calculated by
232 including the carbons from both acetate and gluconate. As for the conditions in T3, cells exhibited a linear,
233 carbon-limited growth pattern throughout the cultivation (Figure 6B). Substrate consumption and WE
234 production were determined at 24 h, where the WE content was found to be higher, reaching 25% of
235 CDW. The productivity was 10 mg WE L⁻¹ h⁻¹, which was expectedly lower compared to T2 due to lower
236 gluconate feeding and subsequently slower cell growth (the CDW was 0.94 g L⁻¹ for T3 at 24 h). However,
237 the specific productivity was found to be similar between T2 and T3, which were 9.0 and 11 mg gCDW⁻¹ h⁻¹
238 ¹, respectively, indicating that the cells were active in WE synthesis despite the reduced gluconate feed
239 rate. Although the WE titer was lower under these conditions compared to that of T2 (240 mg L⁻¹ in T3
240 compared to 340 mgL⁻¹ in T2), the C/C yield was higher, 18%. This was due to slower substrate

241 consumption: 4.4 mM and 31 mM of gluconate and acetate were used at 23 h, respectively (acetate
242 accounted for 68% w/w of total consumed substrates). The T3 cultivation was continued for an additional
243 10 h with the same feed rate. At 33 h, the WE titer had increased from 240 mgL⁻¹ to 290 mgL⁻¹ due to
244 continued cell growth. In addition, the cellular WE content was 26%, which indicates that the cells
245 maintained the cellular WE production rate. Correspondingly, the cells also consumed additional
246 substrates, resulting in a total of 5.7 mM gluconate and 47 mM acetate metabolized (C/C yield was 15%).
247 The proportion of acetate in total substrate consumption was 71% at the 33 h timepoint, close to the
248 optimal substrate ratio predicted by FBA. Additionally, according to FBA, the maximum theoretical C/C
249 yield for WEs from acetate and gluconate are approximately 53% and 57%, respectively, when biomass is
250 not formed. Thus, the experimentally achieved WE yield was approximately 25% of the theoretical
251 maximum for T2 and 33% for T3, although resources were simultaneously directed to biomass. ADP1 WT
252 culture produced significantly less WEs than ADP1m+ cultures: the WE content of the cells was
253 determined to be 3.5% at 12h and 3.1% at 23h. The WE productivity (1 mg L⁻¹h⁻¹), titer (29 mgL⁻¹), or C/C
254 yield (2%) did not change appreciably between the two timepoints. The gluconate and acetate consumed
255 were 3.4 mM and 34 mM (75% w/w acetate), respectively, at the 12 h timepoint, and 5.0 mM and 63 mM
256 (79 % w/w acetate), respectively, at the 23 h timepoint.

257 **Discussion**

258 Microbial lipids have a broad range of potential uses in different industries. Wax esters, for example, can
259 be used as high-quality lubricants, hydraulic oils, as well as pharmaceutical, cosmetic, printing, and food
260 additives. However, efficient microbial production of high-value lipids is still limited by several
261 fundamental challenges. Most important among them is the difficulty in engineering cells for growth-
262 associated lipid production, which would be beneficial from several points of view. Induction of lipid
263 accumulation requires that excess carbon is available but other growth-essential nutrients (i.e. nitrogen)

264 are limited. Such conditions inevitably lead to a trade-off between biomass growth and lipid production.
265 Various strategies to overcome this issue reduce the overall C/C yield and productivity, but can also induce
266 growth inhibition and synthesis of overflow metabolites (Robles-Rodriguez et al., 2018). To address the
267 unfavorable effects of the high C/N ratio, various approaches of metabolic engineering ranging from gene
268 knock-outs, expression of non-native enzymes, engineering redox metabolism, regulation of gene
269 expression, and rewiring pathways have been proposed (Ajjawi et al., 2017; Lazar, Liu, & Stephanopoulos,
270 2018; Lehtinen, et al., 2018; Liang & Jiang, 2013; Santala et al., 2011; Xu, Qiao, Ahn, & Stephanopoulos,
271 2016). Despite improvements at the cellular level, the inherent limitations related to the regulation of
272 lipid synthesis remain.

273 Another issue is the substrate used in most studies targeting lipid production, which is either glucose or
274 other glycolytic compounds. Glucose is undoubtedly a superior substrate for a broad range of production
275 systems, but for societal, economical, and environmental reasons, using more sustainable carbon sources
276 is of high interest. Alternative substrates, such as acetic acid, that are readily available from a variety of
277 renewable sources, potentially inexpensive, and easily metabolizable, should be explored.

278 In the present study, we developed a system to overcome the temporal trade-off between growth and
279 product synthesis in *A. baylyi* ADP1. Our aim was to improve product yield and increase cellular content
280 during active cell growth. We exploited metabolic engineering to partition metabolism into separate
281 modules through *aceA* deletion and overexpression of the native fatty acyl-CoA reductase *acr1*, and used
282 two different substrates, acetate and gluconate, to fuel the metabolic operations of WE synthesis and cell
283 growth, respectively. We confirmed that the carbon from either substrate was retained within their
284 designated parts of metabolism. Thus, our strategy allowed simultaneous and independent control of
285 growth and WE synthesis.

286 Using acetate as the main substrate for *A. baylyi* ADP1 WE synthesis is justified by its single-step
287 conversion into acetyl-CoA, despite the highest reported WE titers (1.8 g L^{-1}) having been obtained with
288 high concentrations (200 mM) of glucose (Luo, et al., 2020). In ADP1, however, glucose and gluconate
289 enter metabolism through a modified Entner-Doudoroff pathway (Kannisto, Aho, Karp, & Santala, 2014).
290 Importantly, the catabolism of glycolytic substrates in *A. baylyi* results in the formation of glyceraldehyde-
291 3-phosphate (G-3-P) and pyruvate. While pyruvate is converted to acetyl-CoA, G-3-P is readily directed to
292 the synthesis of EPS, which are produced through activated sugars generated in gluconeogenesis (Barbe,
293 et al., 2004). Typically, *A. baylyi* produces significant amounts of EPS (~20% of CDW) as overflow
294 metabolites when grown on a surplus of glycolytic substrates (Kaplan & Rosenberg, 1982). High amounts
295 of EPS both complicate product harvesting and cause a significant loss of carbon. Complete elimination of
296 the EPS synthesis route, on the other hand, can result in reduced growth rates and cell aggregation
297 (Kannisto, et al., 2017). Thus, although using high concentrations of glycolytic substrates in *A. baylyi* can
298 increase WE titers, it also leads to a simultaneous reduction in the C/C yield due to byproduct formation.

299 Interestingly, based on the comparative TLC analyses, reducing the gluconate feed by even 8-fold did not
300 negatively affect WE production in ADP1m+ at the cellular level. However, a complete lack of gluconate
301 prevented WE synthesis. This is expected as the engineered cells are incapable of generating the energy
302 and cofactors required for lipid synthesis from acetate alone. For example, the complete TCA cycle is not
303 functional without gluconate, as the replenishment of TCA cycle intermediates is dependent on the
304 carboxylation of phosphoenolpyruvate to oxaloacetate. Taken together, the WE synthesis of ADP1m+ was
305 found to be dependent on the energy and/or cellular building blocks provided by gluconate.

306 FBA analysis was carried out to estimate the effect of varying acetate and gluconate consumption on
307 biomass and WE production. The model predicted that the uptake of 75% acetate and 25% gluconate
308 would simultaneously maximize both WE synthesis and cell growth per used carbon. To experimentally
309 validate this, cultivation in larger scale bioreactors with two different gluconate feed rates were applied.

310 While yield and cellular WE content were higher in T3, the productivity and titer were slightly higher in T2
311 due to lower biomass production in the former. On the other hand, the cells in T2 consumed 3.2 fold more
312 gluconate compared to T3, and the resulting proportion of acetate in total substrate consumption was
313 lower (52% w/w in T2 compared to 68-71% w/w in T3, which was closer to the predicted optimum). Thus,
314 it was both predicted by the model and demonstrated experimentally that a higher gluconate feed rate is
315 beneficial for growth, but reduces the maximal WE accumulation as well as the relative acetate
316 consumption.

317 In ADP1 WT, by contrast, reducing the gluconate feed did not result in higher WE accumulation. The low
318 WE accumulation in these cells was also predicted by FBA, which is consistent with the poor production
319 metrics from acetate observed in our previous study (Santala, et al., 2018). ADP1 WT consumed acetate
320 faster compared to ADP1m+, but acetate was mostly likely directed to biomass through the glyoxylate
321 shunt. This was expected as acetate serves as the preferred carbon source for growth in ADP1, and the
322 cells exhibit higher growth rate with acetate than with glucose (Kannisto et al., 2015). Also, the WT
323 biomass was 26% higher at the end of cultivation compared to ADP1m+, despite similar amounts of
324 gluconate being consumed in both cultivations, further indicating the natural tendency of these cells to
325 divert acetate to biomass. Although the regulation of glyoxylate shunt is not fully understood in
326 *Acinetobacter*, it has been shown that in some strains, the activity of isocitrate lyase is upregulated in the
327 presence of acetate, which can further decrease the flux towards WE synthesis (Cozzone, 1998). With the
328 partitioning of metabolism and increased flux towards WE production in ADP1m+, the cellular WE content
329 and productivity were improved by 7.2 and 4.2 fold, and the product yield and titer were enhanced by 8.3
330 fold, emphasizing the significance of combining the cofeeding and metabolic engineering strategies to
331 fully utilize the efficient acetate metabolism of ADP1.

332 It has been previously shown that among other substrates (such as ethanol and pyruvate and here
333 gluconate), glucose does not repress acetate utilization in ADP1 (Salcedo-Vite, Sigala, Segura, Gosset, &

334 Martinez, 2019). The absence of CCR allows flexible adjustment and optimization of the substrate ratios.
335 Here, optimizing the cofeeding of gluconate and acetate for the engineered strain resulted in the highest
336 reported C/C yield for WE production of 18% (33% of the theoretical maximum, including the carbon
337 required for both cell growth and WE production). In addition, the developed system enables a modular
338 and dynamic process design: by increasing or reducing the gluconate feed, the balance between biomass
339 and product formation can be readily adjusted and optimized. Another interesting approach would be to
340 employ pO₂-coupled feeding strategy at the optimal acetate/gluconate ratio to balance growth and WE
341 synthesis to not only obtain high yields, but also improved titers. Thus, the developed system can provide
342 new possibilities and insights for exploiting fed-batch bioprocesses for microbial lipid production.

343 ADP1m+ cells accumulated most WEs under gluconate-limiting conditions (T3), up to 26% of their CDW.
344 Interestingly, the WE content was maximized already at the 24-hour timepoint, with no significant
345 changes between the 24 and 33-hour timepoints despite continued carbon utilization. WEs within the cell
346 can form intracellular, disk-shaped inclusion bodies, which can have a diameter comparable to that of the
347 cell (Ishige et al., 2002). On the other hand, *Acinetobacter* strains are not, by definition, regarded as
348 oleaginous, because the cellular content of storage lipids does not naturally exceed 20% (Ratledge &
349 Wynn, 2002), with typical wild type strains only achieving approximately 5-10%. Hence, cell functions are
350 possibly disturbed when the WE content exceeds ~25%. Nevertheless, for additional improvements in WE
351 synthesis, engineering an export system for the production of extracellular WEs might be a potential
352 approach. As a result, the designs in this study can further benefit the production metrics of WE once the
353 limitations in cellular WE storage are removed.

354 Combining metabolic engineering with substrate co-feeding was shown to be a simple yet powerful means
355 to control cell operations and optimize carbon flow. Glyoxylate shunt had a key role in distributing carbon
356 between growth and acetyl-CoA-derived products. As the TCA cycle and glyoxylate shunt are highly
357 conserved metabolic routes in microbes, this approach is readily generalizable to other hosts and

358 production systems, with various different substrates. For example, replacing gluconate with more
359 sustainable carbon sources, such as lignin-derived aromatics, could be a feasible alternative for supporting
360 the production of a variety of acetyl-CoA products in *A. baylyi* (Luo, Lehtinen, Efimova, Santala, & Santala,
361 2019; Salmela, Lehtinen, Efimova, Santala, & Santala, 2019; Salmela, Lehtinen, Efimova, Santala, &
362 Santala, 2020). Although CCR can be somewhat restrictive in these applications, limiting the availability of
363 the preferred substrate bypasses the issue and allows cofeeding to be employed universally in many hosts
364 (Park, et al., 2019). While process optimization and scale-up as well as the engineering of a product
365 secretion system are the required next steps in the commercialization of microbial WE production, the
366 described strategy provides a promising means for bypassing fundamental limitations and significantly
367 improving production metrics in lipid-producing hosts.

368 **Conclusions**

369 In this study, the combination of metabolic engineering and substrate cofeeding was introduced to
370 overcome the pressing challenges in microbial lipid production, which manifests in the distribution of
371 resources and time between growth and product synthesis. Dividing the metabolism into two functional
372 units responsible for cell growth and lipid production, respectively, enabled targeted and optimized
373 cofeeding of acetate and gluconate to achieve separate control of these crucial cellular operations. As a
374 result, cells were able to utilize the substrates efficiently for the concurrent synthesis of biomass and wax
375 esters. All production metrics (yield, titer, productivity) and cellular product content were improved by
376 4.2 – 8.3 fold over the control strain. The described engineering approach provides a simple yet effective
377 means to control metabolism and improve production metrics, while being generalizable to various hosts
378 and production systems.

379 **Acknowledgements**

380 The Academy of Finland (no. 310135, 310188, 334822) and the U.S. Department of Energy Genomic
381 Science research program (no. DE-SC0008744) are gratefully acknowledged. We also thank Pauli Losoi for
382 carrying out the flux balance analysis.

383 References

- 384 Ajjawi, I., Verruto, J., Aqui, M., Soriaga, L. B., Coppersmith, J., Kwok, K., . . . Moellering, E. R. (2017). Lipid
385 production in *Nannochloropsis gaditana* is doubled by decreasing expression of a single
386 transcriptional regulator. *Nature biotechnology*, *35*(7), 647-652. doi: 10.1038/nbt.3865
- 387 Barbe, V., Vallenet, D., Fonknechten, N., Kreimeyer, A., Oztas, S., Labarre, L., . . . Médigue, C. (2004).
388 Unique features revealed by the genome sequence of *Acinetobacter* sp. ADP1, a versatile and
389 naturally transformation competent bacterium. *Nucleic Acids Res*, *32*(19), 5766-5779.
- 390 Beopoulos, A., Cescut, J., Haddouche, R., Uribealrea, J.-L., Molina-Jouve, C., & Nicaud, J.-M. (2009).
391 *Yarrowia lipolytica* as a model for bio-oil production. *Progress in Lipid Research*, *48*(6), 375-387.
392 doi: <https://doi.org/10.1016/j.plipres.2009.08.005>
- 393 Burg, J. M., Cooper, C. B., Ye, Z., Reed, B. R., Moreb, E. A., & Lynch, M. D. (2016). Large-scale bioprocess
394 competitiveness: the potential of dynamic metabolic control in two-stage fermentations. *Current*
395 *Opinion in Chemical Engineering*, *14*, 121-136. doi: <https://doi.org/10.1016/j.coche.2016.09.008>
- 396 Cozzone, A. J. (1998). REGULATION OF ACETATE METABOLISM BY PROTEIN PHOSPHORYLATION IN
397 ENTERIC BACTERIA. *Annual Review of Microbiology*, *52*(1), 127-164. doi:
398 10.1146/annurev.micro.52.1.127
- 399 Durot, M., Le Fèvre, F., de Berardinis, V., Kreimeyer, A., Vallenet, D., Combe, C., . . . Schachter, V. (2008).
400 Iterative reconstruction of a global metabolic model of *Acinetobacter baylyi* ADP1 using high-
401 throughput growth phenotype and gene essentiality data. *BMC Syst Biol*, *2*, 85.
- 402 Ebrahim, A., Lerman, J. A., Palsson, B. O., & Hyduke, D. R. (2013). COBRApy: CONstraints-Based
403 Reconstruction and Analysis for Python. *BMC Systems Biology*, *7*(1), 74. doi: 10.1186/1752-0509-
404 7-74
- 405 Fixter, L. M., Nagi, M. N., McCormack, J. G., & Fewson, C. A. (1986). Structure, Distribution and Function
406 of Wax Esters in *Acinetobacter calcoaceticus* *Journal of General Microbiology* *132*, 3147-3157.
- 407 Hartmans, S., Smits, J. P., van der Werf, M. J., Volkering, F., & de Bont, J. A. (1989). Metabolism of Styrene
408 Oxide and 2-Phenylethanol in the Styrene-Degrading *Xanthobacter* Strain 124X. *Applied and*
409 *environmental microbiology*, *55*(11), 2850-2855.
- 410 Ishige, T., Tani, A., Sakai, Y., & Kato, N. (2003). Wax ester production by bacteria. *Curr Opin Microbiol*, *6*(3),
411 244-250.
- 412 Ishige, T., Tani, A., Takabe, K., Kawasaki, K., Sakai, Y., & Kato, N. (2002). Wax ester production from n-
413 alkanes by *Acinetobacter* sp. strain M-1: ultrastructure of cellular inclusions and role of acyl
414 coenzyme A reductase. *Appl Environ Microbiol*, *68*(3), 1192-1195.
- 415 Kannisto, M., Aho, T., Karp, M., & Santala, V. (2014). Metabolic engineering of *Acinetobacter baylyi* ADP1
416 for improved growth on gluconate and glucose. *Appl Environ Microbiol*, *80*(22), 7021-7027. doi:
417 10.1128/AEM.01837-14
- 418 Kannisto, M., Efimova, E., Karp, M., & Santala, V. (2017). Growth and wax ester production of an
419 *Acinetobacter baylyi* ADP1 mutant deficient in exopolysaccharide capsule synthesis. *J Ind*
420 *Microbiol Biotechnol*, *44*(1), 99-105. doi: 10.1007/s10295-016-1872-1
- 421 Kannisto, M. S., Mangayil, R. K., Shrivastava-Bhattacharya, A., Pletschke, B. I., Karp, M. T., & Santala, V. P.
422 (2015). Metabolic engineering of *Acinetobacter baylyi* ADP1 for removal of *Clostridium butyricum*

423 growth inhibitors produced from lignocellulosic hydrolysates. *Biotechnology for biofuels*, 8(1), 1-
424 10. doi: 10.1186/s13068-015-0389-6

425 Kaplan, N., & Rosenberg, E. (1982). Exopolysaccharide Distribution of and Bioemulsifier Production by
426 *Acinetobacter calcoaceticus* BD4 and BD413. *Appl Environ Microbiol*, 44(6), 1335-1341.

427 Kent, R., & Dixon, N. (2020). Contemporary Tools for Regulating Gene Expression in Bacteria. *Trends in*
428 *biotechnology*, 38(3), 316-333. doi: <https://doi.org/10.1016/j.tibtech.2019.09.007>

429 Kurosawa, K., Boccazzi, P., de Almeida, N. M., & Sinskey, A. J. (2010). High-cell-density batch fermentation
430 of *Rhodococcus opacus* PD630 using a high glucose concentration for triacylglycerol production.
431 *Journal of Biotechnology*, 147(3-4), 212-218. doi: 10.1016/j.jbiotec.2010.04.003

432 Lalwani, M. A., Zhao, E. M., & Avalos, J. L. (2018). Current and future modalities of dynamic control in
433 metabolic engineering. *Current Opinion in Biotechnology*, 52, 56-65. doi:
434 10.1016/j.copbio.2018.02.007

435 Lazar, Z., Liu, N., & Stephanopoulos, G. (2018). Holistic Approaches in Lipid Production by *Yarrowia*
436 *lipolytica*. *Trends in biotechnology*, 36(11), 1157-1170. doi:
437 <https://doi.org/10.1016/j.tibtech.2018.06.007>

438 Lehtinen, T., Efimova, E., Santala, S., & Santala, V. (2018). Improved fatty aldehyde and wax ester
439 production by overexpression of fatty acyl-CoA reductases. *Microbial Cell Factories*, 17(1), 19. doi:
440 10.1186/s12934-018-0869-z

441 Liang, M. H., & Jiang, J. G. (2013). Advancing oleaginous microorganisms to produce lipid via metabolic
442 engineering technology. *Progress in Lipid Research*, 52(4), 395-408. doi:
443 10.1016/j.plipres.2013.05.002

444 Lo, T.-M., Chng, S. H., Teo, W. S., Cho, H.-S., & Chang, M. W. (2016). A Two-Layer Gene Circuit for
445 Decoupling Cell Growth from Metabolite Production. *Cell Systems*, 3(2), 133-143. doi:
446 <https://doi.org/10.1016/j.cels.2016.07.012>

447 Luo, J., Efimova, E., Losoi, P., Santala, V., & Santala, S. (2020). Wax ester production in nitrogen-rich
448 conditions by metabolically engineered *Acinetobacter baylyi* ADP1. *Metabolic Engineering*
449 *Communications*, e00128. doi: <https://doi.org/10.1016/j.mec.2020.e00128>

450 Luo, J., Lehtinen, T., Efimova, E., Santala, V., & Santala, S. (2019). Synthetic metabolic pathway for the
451 production of 1-alkenes from lignin-derived molecules. *Microbial Cell Factories*, 18(1), 48. doi:
452 10.1186/s12934-019-1097-x

453 Lv, Y., Qian, S., Du, G., Chen, J., Zhou, J., & Xu, P. (2019). Coupling feedback genetic circuits with growth
454 phenotype for dynamic population control and intelligent bioproduction. *Metabolic engineering*,
455 54, 109-116. doi: <https://doi.org/10.1016/j.ymben.2019.03.009>

456 Mehrer, C. R., Rand, J. M., Incha, M. R., Cook, T. B., Demir, B., Motagamwala, A. H., . . . Pfleger, B. F. (2019).
457 Growth-coupled bioconversion of levulinic acid to butanone. *Metabolic engineering*, 55, 92-101.
458 doi: 10.1016/j.ymben.2019.06.003

459 Park, J. O., Liu, N., Holinski, K. M., Emerson, D. F., Qiao, K., Woolston, B. M., . . . Stephanopoulos, G. (2019).
460 Synergistic substrate cofeeding stimulates reductive metabolism. *Nature Metabolism*, 1, 643-651.

461 Ratledge, C., & Wynn, J. P. (2002). The Biochemistry and Molecular Biology of Lipid Accumulation in
462 Oleaginous Microorganisms. In A. I. Laskin, J. W. Bennett & G. M. Gadd (Eds.), *Advances in applied*
463 *microbiology* (Vol. 51, pp. 1-52): Academic Press.

464 Reiser, S., & Somerville, C. (1997). Isolation of mutants of *Acinetobacter calcoaceticus* deficient in wax
465 ester synthesis and complementation of one mutation with a gene encoding a fatty acyl coenzyme
466 A reductase. *J Bacteriol*, 179(9), 2969-2975.

467 Robles-Rodriguez, C. E., Munoz-Tamayo, R., Bideaux, C., Gorret, N., Guillouet, S. E., Molina-Jouve, C., . . .
468 Aceves-Lara, C. A. (2018). Modeling and optimization of lipid accumulation by *Yarrowia lipolytica*
469 from glucose under nitrogen depletion conditions. *Biotechnology and bioengineering*, 115(5),
470 1137-1151. doi: 10.1002/bit.26537

- 471 Salcedo-Vite, K., Sigala, J. C., Segura, D., Gosset, G., & Martinez, A. (2019). *Acinetobacter baylyi* ADP1
472 growth performance and lipid accumulation on different carbon sources. *Applied Microbiology
473 and Biotechnology*, 103(15), 6217-6229. doi: 10.1007/s00253-019-09910-z
- 474 Salmela, M., Lehtinen, T., Efimova, E., Santala, S., & Santala, V. (2019). Alkane and wax ester production
475 from lignin-related aromatic compounds. *Biotechnology and bioengineering*, 116(8), 1934-1945.
476 doi: 10.1002/bit.27005
- 477 Salmela, M., Lehtinen, T., Efimova, E., Santala, S., & Santala, V. (2020). Towards bioproduction of poly- α -
478 olefins from lignocellulose. *Green Chemistry*, 22(15), 5067-5076. doi: 10.1039/d0gc01617a
- 479 Santala, S., Efimova, E., Kivinen, V., Larjo, A., Aho, T., Karp, M., & Santala, V. (2011). Improved
480 triacylglycerol production in *Acinetobacter baylyi* ADP1 by metabolic engineering. *Microb Cell
481 Fact*, 10, 36. doi: 10.1186/1475-2859-10-36
- 482 Santala, S., Efimova, E., Koskinen, P., Karp, M. T., & Santala, V. (2014). Rewiring the wax ester production
483 pathway of *Acinetobacter baylyi* ADP1. *ACS Synth Biol*, 3(3), 145-151. doi: 10.1021/sb4000788
- 484 Santala, S., Efimova, E., & Santala, V. (2018). Dynamic decoupling of biomass and wax ester biosynthesis
485 in *Acinetobacter baylyi* by an autonomously regulated switch. *Metabolic Engineering
486 Communications*, 7, e00078. doi: <https://doi.org/10.1016/j.mec.2018.e00078>
- 487 Stöveken, T., Kalscheuer, R., Malkus, U., Reichelt, R., & Steinbüchel, A. (2005). The wax ester synthase/acyl
488 coenzyme A:diacylglycerol acyltransferase from *Acinetobacter* sp. strain ADP1: characterization
489 of a novel type of acyltransferase. *J Bacteriol*, 187(4), 1369-1376. doi: 10.1128/JB.187.4.1369-
490 1376.2005
- 491 von Kamp, A., & Klamt, S. (2017). Growth-coupled overproduction is feasible for almost all metabolites in
492 five major production organisms. *Nature Communications*, 8. doi: Artn 15956
493 10.1038/Ncomms15956
- 494 Xu, J. Y., Zhao, X. B., Du, W., & Liu, D. H. (2017). Bioconversion of glycerol into lipids by *Rhodospiridium*
495 *toruloides* in a two-stage process and characterization of lipid properties. *Engineering in Life
496 Sciences*, 17(3), 303-313. doi: 10.1002/elsc.201600062
- 497 Xu, P., Qiao, K., Ahn, W. S., & Stephanopoulos, G. (2016). Engineering *Yarrowia lipolytica* as a platform for
498 synthesis of drop-in transportation fuels and oleochemicals. *Proceedings of the National Academy
499 of Sciences*, 113(39), 10848-10853. doi: 10.1073/pnas.1607295113
- 500 Yan, Q., & Pflieger, B. F. (2020). Revisiting metabolic engineering strategies for microbial synthesis of
501 oleochemicals. *Metabolic engineering*, 58, 35-46. doi: 10.1016/j.ymben.2019.04.009

502

503

504

505

506

507

508 **Figure legends**

509 **Figure 1. Dividing metabolism for simultaneous biomass and product synthesis.** A) Conventionally, lipid
510 production is carried out in two phases, growth and lipid synthesis. Lipid accumulation is induced in the
511 stationary phase by providing excess carbon and limiting growth-essential nutrients, such as nitrogen. B)
512 By dividing the cells' metabolism into two separate units, different parts of metabolism can be
513 independently controlled using multiple substrates. As a result, the cells can simultaneously grow and also
514 synthesize lipids.

515

516 **Figure 2. Production of biomass and wax esters as well as the consumption of acetate and gluconate by**
517 **ADP1 WT and ADP1m+.** The strains were cultivated in shake flasks using minimal salts medium
518 supplemented with 100 mM gluconate and 100 mM acetate for 48 hours. A) The optical density (OD_{600}) of
519 the culture was used to determine biomass and the consumption of acetate and gluconate were measured
520 by HPLC. The data is shown as an average of two biologically independent replicates and the error bars
521 represent standard deviation. Filled symbols – ADP1m+, empty symbols – ADP1 wt. B) WE production was
522 determined by comparative TLC analysis at 31- and 47-hour timepoints for ADP1 WT and ADP1m+.
523 Samples from two biologically independent cultures were analyzed on separate HPTLC plates. Jojoba oil
524 was used as the standard (std).

525

526 **Figure 3. Distribution of carbons from gluconate and acetate among various pathways in ADP1m+.** The
527 strain ADP1m+ was cultivated in MSM supplemented with [$U-^{13}C_2$]Na-acetate and natural-abundance Na-
528 gluconate. Both carbon sources were available in excess at the time of sampling. The average degree of
529 labelling for each compound is indicated by color (red - fully labelled, blue – unlabeled, $n = 5$). The

530 *intermediates of glycolysis and the pentose phosphate pathway were exclusively contributed by gluconate,*
531 *whereas $\geq 90\%$ lipids were produced from acetate. Pyr, pyruvate; Cit, citrate; aKG, alphaketoglutarate;*
532 *Fum, fumarate; Mal, malate; OA, oxaloacetate; PEP, phosphoenolpyruvate; Gly3P, glyceraldehyde-3-*
533 *phosphate; DHAP, dihydroxyacetone phosphate; F6P, fructose-6-phosphate; R5P, ribulose-5-phosphate.*

534

535 **Figure 4. Growth and wax ester production of ADP1m+ from acetate and gluconate at different**
536 **gluconate feeding rates.** *The engineered strain ADP1m+ was cultivated in MSM containing 70-100 mM*
537 *acetate, while gluconate was gradually introduced at different feed rates (0.8 mM h^{-1} , 0.4 mM h^{-1} , 0.2 mM*
538 *h^{-1} , 0.1 mM h^{-1}). Growth was determined based on the optical density (OD_{600}) and gluconate and acetate*
539 *concentrations were determined by HPLC. The data is shown as an average of two replicates and the error*
540 *bars represent standard deviation (error bars not visible in all data points). Despite the excess acetate*
541 *available in the culture, cells exhibited carbon-limited growth when gluconate was fed at limiting*
542 *quantities. Total consumptions of acetate and gluconate (Ace ; Glcn mM) are presented for each culture.*
543 *Higher gluconate availability resulted in increased absolute substrate consumptions (both acetate and*
544 *gluconate), but more acetate was consumed relative to gluconate with lower feed rates. Higher gluconate*
545 *feeding allowed the cells to grow better, but WE production did not increase, as demonstrated by*
546 *comparative TLC analysis.*

547

548 **Figure 5. Segregated metabolism requires both gluconate and acetate for the synthesis of biomass and**
549 **wax esters.** *It was experimentally determined that cells could not grow or maintain essential operations*
550 *without gluconate. On the other hand, acetate was required for WE synthesis in the studied conditions, as*
551 *demonstrated by TLC analyses. The lipid samples were taken from cultivations carried out in MSM*

552 supplemented with 0.4 mM h^{-1} gluconate feed, with and without 75 mM acetate. G – gluconate; A –
553 acetate; WE – wax ester.

554

555 **Figure 6. Growth and wax ester production of ADP1m+ in bioreactors with two different gluconate feed**
556 **rates.** The strain ADP1m+ was cultivated in MSM supplemented with 50-75 mM acetate. A feed stream
557 containing a mixture of gluconate and acetic acid (both at same concentration) at a rate of 0.6 mM h^{-1} (A;
558 T2) or 0.1 mM h^{-1} (B; T3) was also implemented. Partial oxygen pressure was set to $\geq 20\%$, and pH to 7.5.
559 Dashed lines indicate the time of sampling for WE analyses (22 h for T2, 24 h for T3), for which the results
560 are presented in C). Wax esters were quantified using NMR, and cellular WE content (WE/biomass, %), C/C
561 yield (%), productivity ($\text{mg L}^{-1} \text{ h}^{-1}$), and titer (mg L^{-1}) were calculated. ADP1 WT was cultivated in conditions
562 similar to T3 (for details, see Supplementary Figure S7), but for comparable samples, results of the 12-hour
563 timepoint sample is shown. The data is shown as an average of two replicates and the error bars represent
564 standard deviation.

565

Figure 1.

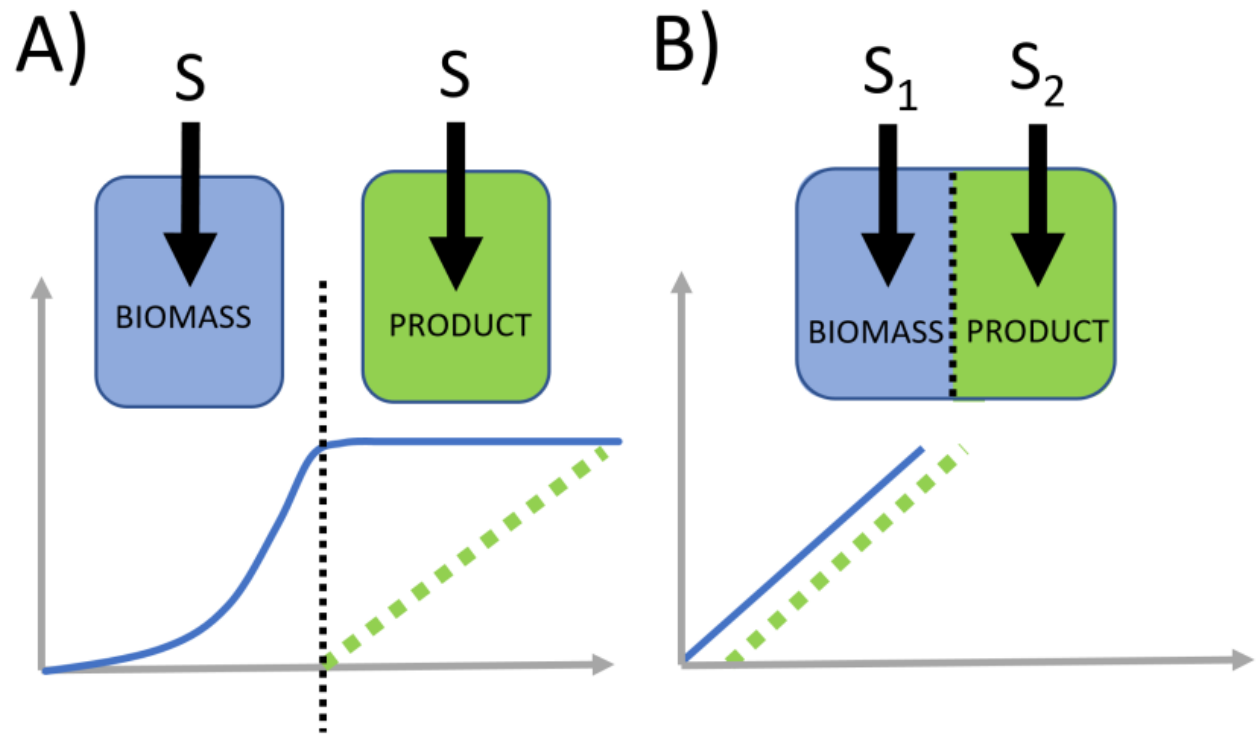


Figure 2.

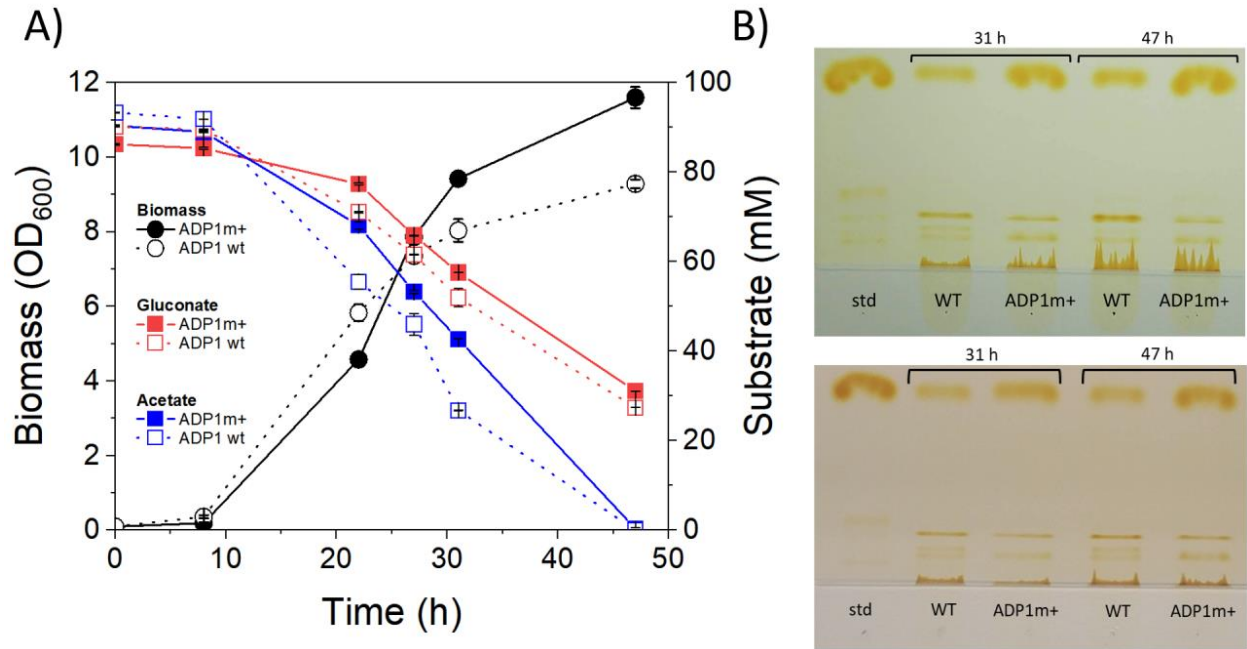


Figure 3.

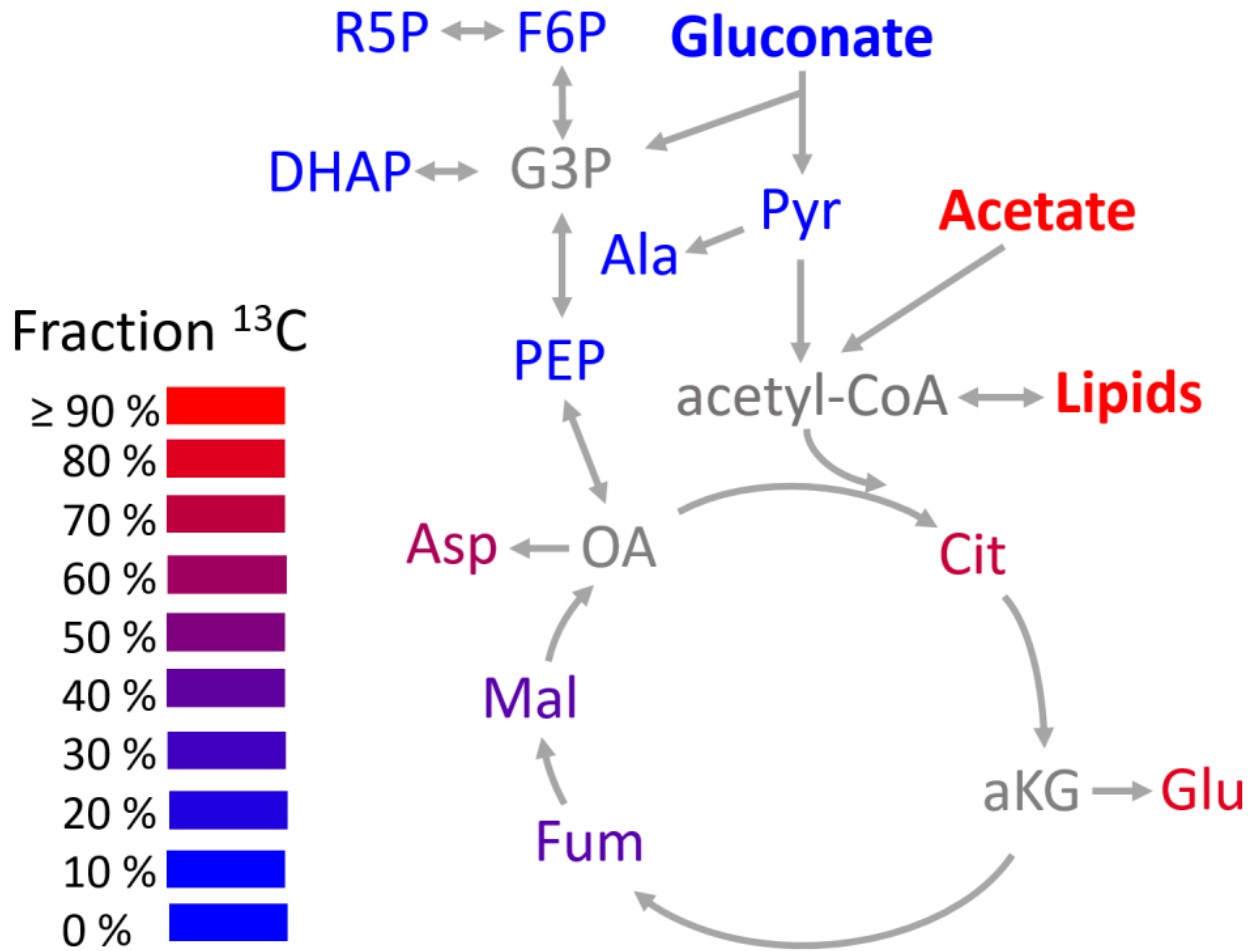


Figure 4.

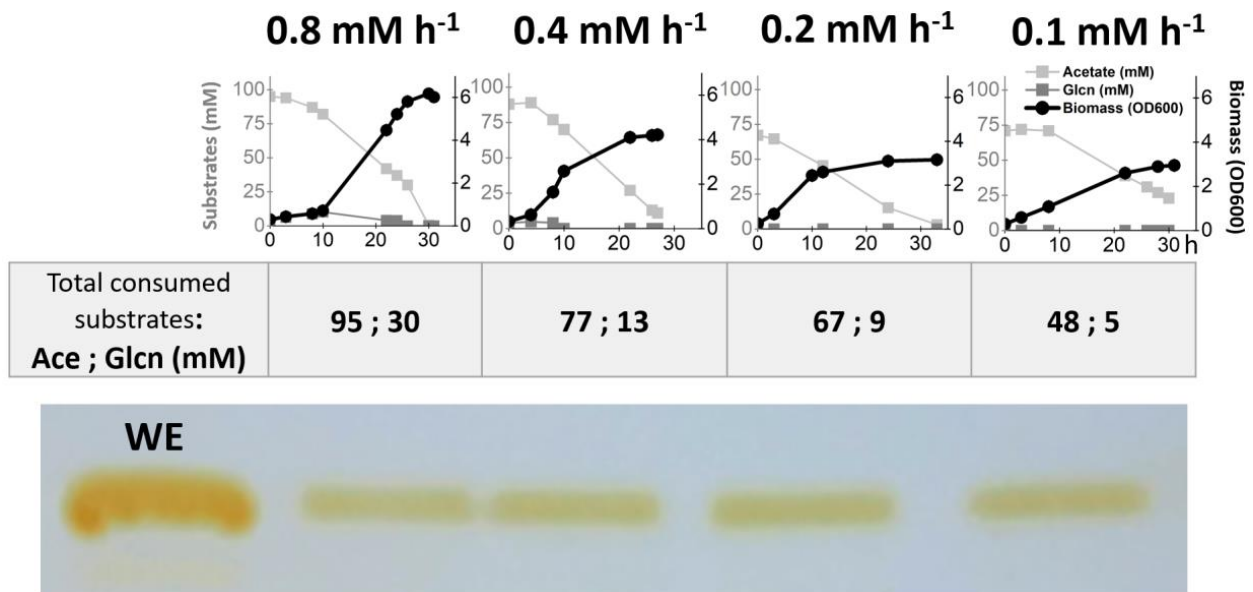


Figure 5.







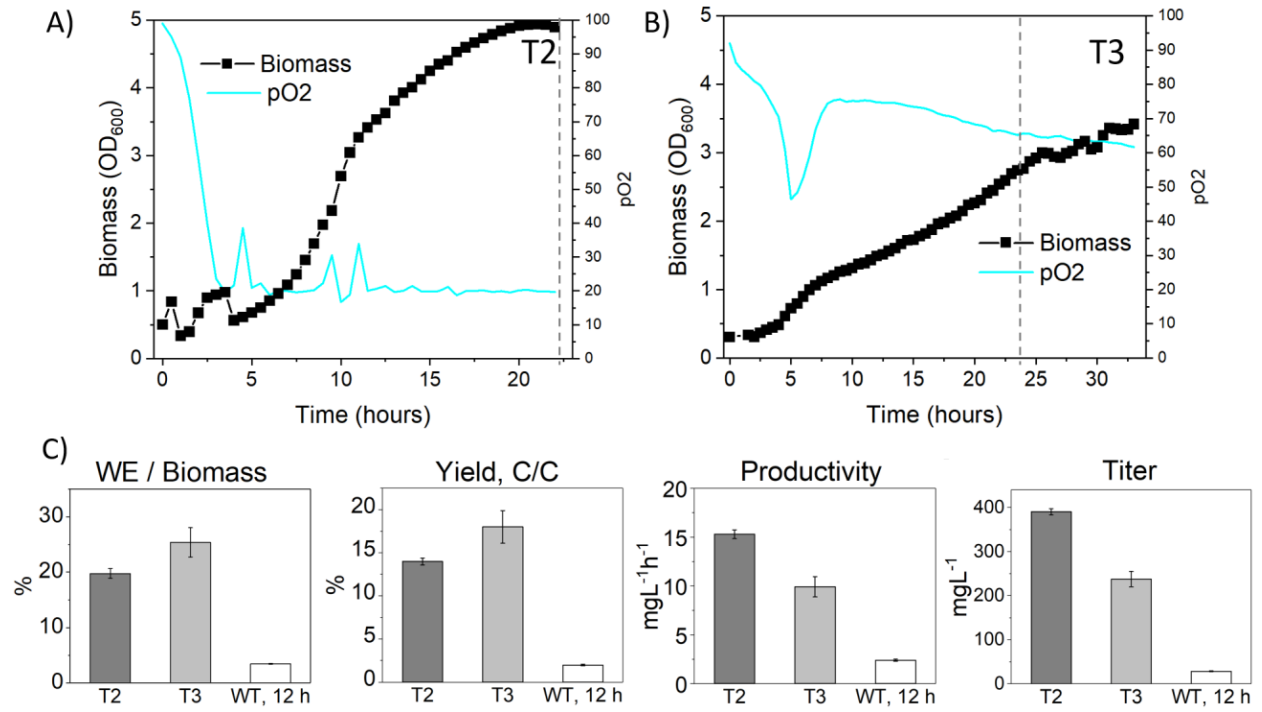
INPUT		OUTPUT	
G	A	Growth	WE
0	0	0 	0
0	1	0 	0
1	0	1 	0 
1	1	1 	1 

Figure 6.



Supplementary information for

Partitioning metabolism between growth and product synthesis for coordinated production of wax esters in *Acinetobacter baylyi* ADP1

Suvi Santala^{1,2}, Ville Santala^{1,2}, Nian Liu¹, and Gregory Stephanopoulos^{1*}

¹Department of Chemical Engineering, Massachusetts Institute of Technology, Cambridge, MA 02139

²Faculty of Engineering and Natural Sciences, Tampere University, Hervanta Campus, 33720 Tampere, Finland

*Corresponding author gregstep@mit.edu

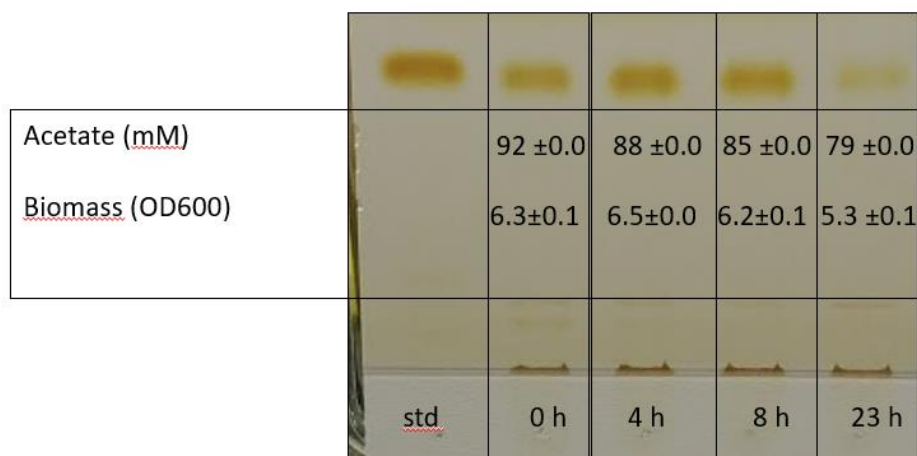


Figure S1. Utilization of acetate and production of WEs by ADP1m+ without gluconate. The strain ADP1m+ was first cultivated in MSM supplemented with 100 mM acetate and 100 mM gluconate. After 22 hours, the cells were collected by centrifugation at 4000 g for 30 mins, and suspended to MSM medium supplemented with ~100 mM acetate, and incubated for 23 hours at 30°C. Biomass was determined as optical density (OD600), and substrate utilization and WE production were determined by HPLC and comparative TLC analyses, respectively. The WE band detected at 0-hour timepoint represents the WEs produced in the first cultivation phase. Despite the substantial amount of biomass in the beginning of the culture, the cells consumed only ~13 mM of acetate during the 23-hour cultivation, implying that the cells are not able to maintain acetate utilization and WE synthesis after the cells run out of resources for lipid synthesis; At 4- and 8-hour timepoints, slight increase in WEs is detected, whereas at 23 hours, the amount of both biomass (OD600) and WEs have reduced.

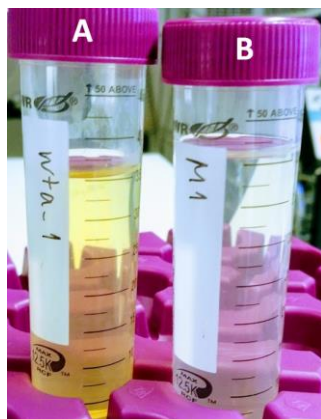


Figure S2. Visual inspection of supernatants from gluconate limiting and non-limiting cultivations. The cells were removed by centrifugation (4500 g, 30 min at 4°C) and the supernatants were transferred to clean tubes. The tube on the left (A) contains the supernatant from batch cultivation with both substrates (100 mM gluconate and 100 mM acetate) in excess. The right-side tube (B) contains the supernatant from the cultivation under gluconate limiting conditions with excess acetate (100 mM initially).

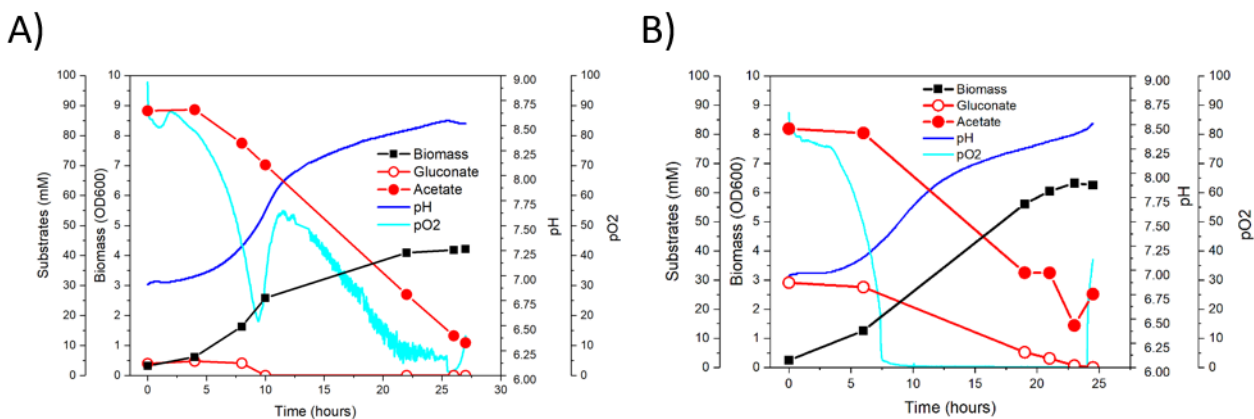


Figure S3. Growth and substrate utilization of ADP1m+ in small-scale reactor. Data for two cultivations with different gluconate feeding rates are presented as examples. The strain ADP1m+ was cultivated in MSM supplemented with 80-90 mM acetate and gluconate fed at rate 0.4 mMh⁻¹ (A) and 0.8 mMh⁻¹ (B). In (A), gluconate-limited growth is detected as reduced growth rate and increased partial oxygen pressure, as well as lower OD at end-point. In B), due to higher gluconate feeding rate, gluconate is available in excess for cells until the end of cultivation, resulting in higher OD and oxygen limitation.

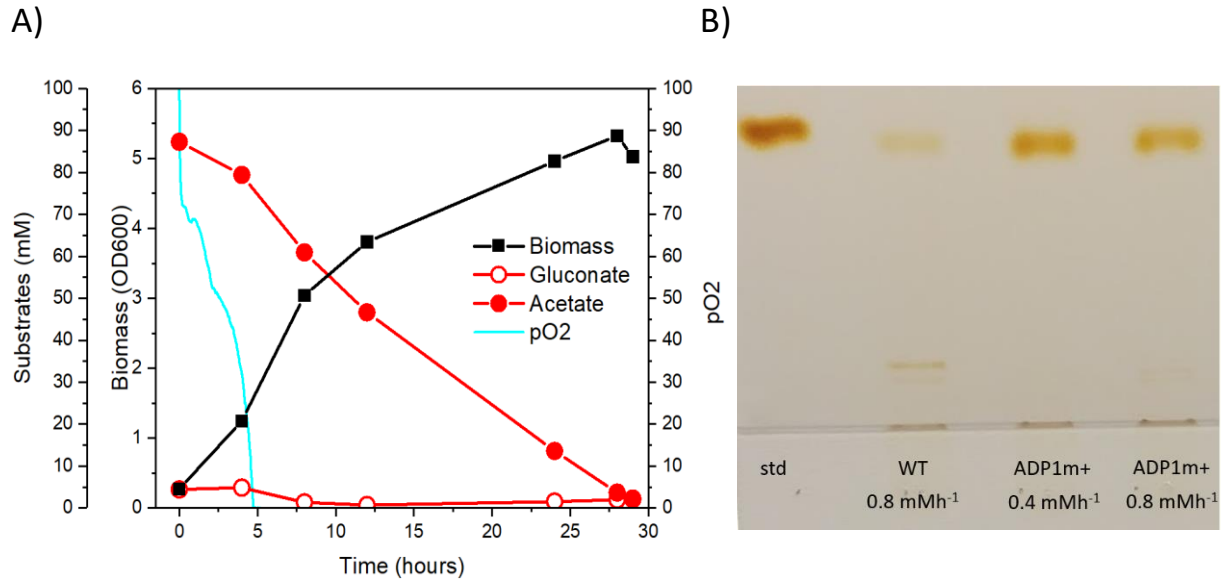


Figure S4. Performance of ADP1 WT in small-scale reactor. A) Growth and substrate utilization of ADP1 WT. The cells were cultivated in MSM supplemented with 90 mM acetate and gluconate at feeding rate 0.8 mMh⁻¹. Biomass was determined as optical density (OD600) and substrate consumption was determined by HPLC. Due to excess carbon, the cells rapidly consumed the oxygen (pO₂) and shifted to oxygen-limited growth mode. B) Thin layer chromatography analysis of wax esters produced by ADP1 WT. Samples from ADP1m+ cultivations at gluconate feed 0.4 mMh⁻¹ and 0.8 mMh⁻¹ (Figure S3) were used as reference and jojoba oil was used as the standard (std). Equal volumes of culture samples were taken for the analysis.

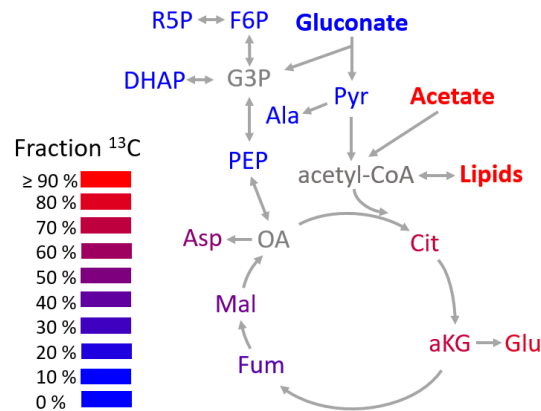


Figure S5. Distribution of carbon to different pathways in ADP1m+. The strain ADP1m+ was cultivated in MSM supplemented with [¹³C₂]-labelled Na-acetate and natural-abundance Na-gluconate. Cultivation was carried out in gluconate-limiting conditions with [¹³C₂] Na-acetate available in excess. The mean of degree of labelling for each compound is indicated by color (red - fully labelled, blue – unlabeled, n = 8). The intermediates of glycolysis and the pentose phosphate pathway are exclusively contributed by gluconate, whereas ≥ 90% lipids are produced from acetate. Pyr, pyruvate; Cit, citrate; aKG, alphaketoglutarate; Fum, fumarate; Mal, malate; OA, oxaloacetate; PEP, phosphoenolpyruvate; Gly3P, glyceraldehyde-3-phosphate; DHAP, dihydroxyacetone phosphate; F6P, fructose-6-phosphate; R5P, ribulose-5-phosphate.

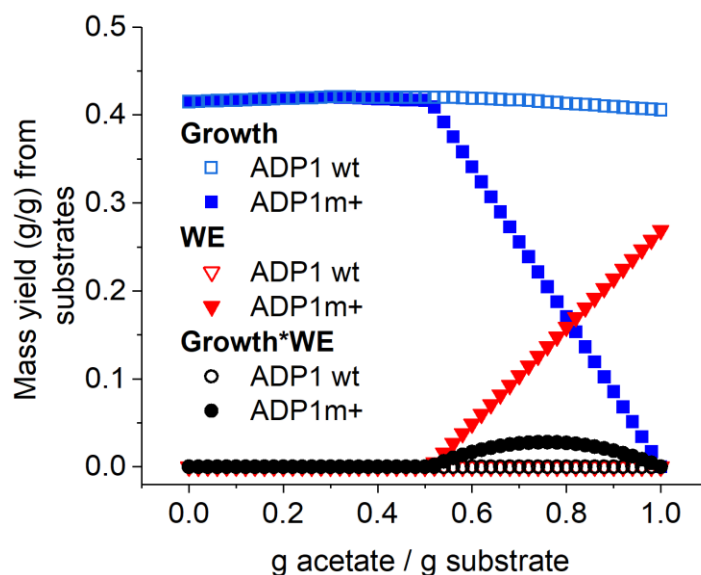


Figure S6. Flux balance analysis for growth and wax ester (WE) production of ADP1 WT and ADP1m+ using acetate and gluconate as carbon sources. A maximum of $1 \text{ gCDW}^{-1} \text{ h}^{-1}$ total substrate was used as an input. A wax ester production 0.01 (g/g) is integrated in the model as default. In the figure, WE production represents the extra accumulation resulting from residual carbon source not directed to biomass synthesis.

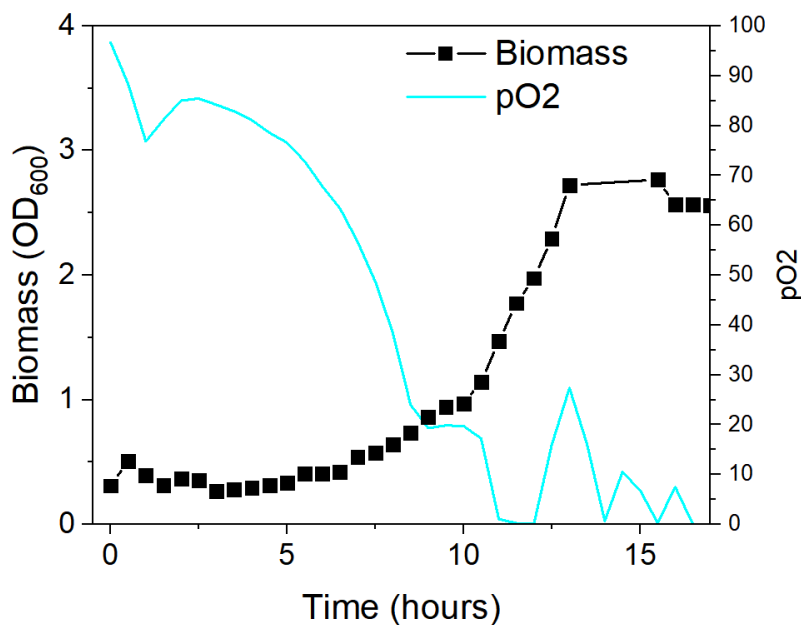


Figure S7. Growth of ADP1 WT in a bioreactor. The strain ADP1 WT was cultivated in MSM supplemented with 75 mM acetate and a feed containing gluconate and acetic acid, which was fed at rate 0.1 mMh^{-1} . In the culture, pH was set to 7.5 and partial oxygen pressure to 20% by a stirring cascade. Sample for WE analysis was taken at 12-hour timepoint (see the main text). Cells exhibited exponential growth despite gluconate limitation.

Lipid analyses

To determine the ^{13}C isotopically labelled fraction of the fatty acids produced by ADP1m+, lipids were extracted, transesterified to fatty acid methyl esters (FAME), and analyzed using gas chromatography-mass spectrometry (GC-MS) (Agilent) as described previously (Park et al., 2019). Briefly, 1-2 ml culture containing ~1 mg biomass was taken for extraction. The samples were centrifuged for 5 mins at 16,000g and the supernatant was discarded. Methyl decanoate (Sigma) and glyceryl triheptadecanoate (Sigma) in hexane (2 mg ml^{-1}) were used as internal standards. Transesterification was carried out in 0.5 N sodium methoxide solution (500 μl per sample) with vortexing at 1,200 rpm for 60 min. 40 μl of 98% sulfuric acid was added to each sample and 500 μl of hexane was used for extracting the FAMEs. Additional vortexing at 1,200 rpm for 30 min was carried out, followed by centrifugation at 6,000g for 1 min. The hexane layer was transferred to another vial and the solvent was evaporated under N_2 . The lipid samples containing FAMEs were resuspended in 50 μl of hexane and 1 μl of the sample was injected into an Agilent 7890B GC coupled to a 5977B MS detector. HP-5ms (Agilent Technologies) was used as the separation column, which was held initially at 165 $^\circ\text{C}$ for 2 min, ramped up to 226 $^\circ\text{C}$ at 2 $^\circ\text{C}/\text{min}$, and then held at that temperature for 1 min. Helium was used as the carrier gas (2 ml min^{-1}). The injection temperature was set to 280 $^\circ\text{C}$. The MS was set to scan m/z values ranging between 200 and 400. The source and quadrupole temperatures were held at 280 $^\circ\text{C}$ and 150 $^\circ\text{C}$, respectively. All isotopic enrichment results were corrected for natural abundance. For other experiments, the amount of total lipids was determined gravimetrically and the amount of produced WEs were estimated by TLC or quantified by NMR. For TLC, lipids were extracted from culture samples (1-3 ml) using the chloroform-methanol extraction as described previously (Lehtinen, Efimova, Santala, & Santala, 2018). Thirty μl of the (lower) chloroform phase was applied to 20 \times 10 cm Silica Gel 60 F254 HPTLC glass plates with a 2.5 \times 10 cm concentrating zone (Merck, USA). The mobile phase was a mixture of n-hexane, diethyl ether, and acetic acid at a ratio of 90:15:1 and iodine was used for visualization. Jojoba oil was used as the standard for WEs. For ^1H NMR analysis, lipids were

extracted from 20-50 mg freeze-dried biomass samples as described previously (Santala, Efimova, Karp, & Santala, 2011). The areas of the peaks in the NMR spectrum are directly proportional to the molar concentration of each functional group, yielding the specific concentration for WEs in total biomass. The concentration of WEs was calculated from the integrated signal at 4.05 ppm which is characteristic for protons of the α -alkoxy-methylene group of esters ($-\text{CH}_2\text{-COO-CH}_2-$). For calculation of the WE titer in grams per liter, an average molar mass of 506 g mol^{-1} was used, based on GC analyses and the average chain length determined from NMR-spectra (Lehtinen, et al., 2018).

Substrate and metabolite analyses

Intracellular metabolites were extracted as described previously (Park, et al., 2019). Briefly, the cells were collected during the exponential ($\text{OD} \sim 0.3$) or carbon-limited ($\text{OD} \sim 1$) growth phases, filtered, and transferred to a cold 40:40:20 acetonitrile/methanol/water solution. After 20 min incubation at $-20 \text{ }^\circ\text{C}$, the filters were washed, the solutions were centrifuged, then the supernatants were divided into two aliquots (LC-MS and GC-MS) and dried under nitrogen. For the LC-MS analysis, the dried samples were resuspended in $50 \text{ }\mu\text{L}$ water and analyzed on a Agilent 1100 Series HPLC system (Agilent Technologies) with a XBridge C18 ($3.5 \text{ }\mu\text{m}$ particle size) $150 \times 2.1 \text{ mm}$ column (Waters) coupled to an API 4000 MS/MS (AB Sciex) by electrospray ionization. With 10 mM tributylamine, 15 mM acetic acid as solvent A and acetonitrile as solvent B, the chromatographic mobile phase was run at a total flow rate of 0.3 ml min^{-1} with the following gradient: 0% B for 8 min; from 0% to 22.5% B between 8 min and 18 min; from 22.5% to 40% B between 18 min and 28 min; from 40% to 60% B between 28 min and 32 min; from 60% to 90% B between 32 min and 34 min; held at 90% B between 34 min and 36 min; from 90% to 100% B between 36 min and 37 min; held at 100% B between 37 min and 42 min. The mass spectrometer was operated in multiple reaction monitoring (MRM) mode. For GC-MS analysis, the dried samples were resuspended in $20 \text{ }\mu\text{L}$ 2% methoxyamine-hydrogen chloride in pyridine (MOX Reagent, Thermo Scientific) and heated to $37 \text{ }^\circ\text{C}$ for 90 min. Afterwards, $25 \text{ }\mu\text{L}$ N-tert-butyldimethylsilyl-N-methyltrifluoroacetamide with 1% tert-

butyldimethylchlorosilane (TBDMS, Sigma-Aldrich) was added and the samples were heated to 56 °C for 60 min. After centrifugation, 3 µL of the supernatant was injected to an Agilent 6890N GC coupled to a 5975B MSD (Agilent Technologies). A J&W DB-35ms column was used with helium as the carrier gas (1 mL min⁻¹). The column temperature was set at 100 °C initially for 1 min, increased to 105 °C at 2.5 °C/min, held at 105 °C for 2 min, increased to 250 °C at 3.5 °C/min, and increased to 320 °C at 20 °C/min. The injection temperature was set to 270 °C. The MS operated in selective ion monitoring (SIM) mode and the source and quadrupole temperatures were 230 °C and 150 °C, respectively. All isotopic enrichment results.

Gluconate and acetate concentrations in batch and small-scale reactor cultivations were analyzed on an Agilent 1200 HPLC system with a Refractive Index Detector (Agilent Technologies). Centrifugation (16,000 g, 5 min) and filtering (with 0.2 µm filters) were carried out prior to injection, which was done using a volume of 10 µL. An HPX-87H column (Bio-Rad Laboratories) was used for separation and 14 mM sulfuric acid was used as the mobile phase at a flow rate of 0.7 mL min⁻¹. For large scale bioreactor cultivations, samples were analyzed using a LC-20AC prominence liquid chromatography system (Shimadzu, USA) equipped with a RID-10A refractive index detector. A Phenomenex Rezex RHM-monosaccharide H+ (8%) column (Phenomenex) was used and 0.01 N sulfuric acid was used as a mobile phase with a flow rate 0.6 mL min⁻¹.

References

- Lehtinen, T., Efimova, E., Santala, S., & Santala, V. (2018). Improved fatty aldehyde and wax ester production by overexpression of fatty acyl-CoA reductases. *Microbial Cell Factories*, *17*(1), 19. doi: 10.1186/s12934-018-0869-z
- Park, J. O., Liu, N., Holinski, K. M., Emerson, D. F., Qiao, K., Woolston, B. M., . . . Stephanopoulos, G. (2019). Synergistic substrate cofeeding stimulates reductive metabolism. *Nature Metabolism*, *1*, 643-651.
- Santala, S., Efimova, E., Karp, M., & Santala, V. (2011). Real-time monitoring of intracellular wax ester metabolism. *Microb Cell Fact*, *10*, 75. doi: 10.1186/1475-2859-10-75